Retinal oximeter for the blue-green oximetry technique

Kurt R. Denninghoff
Katarzyna B. Sieluzycka
Jennifer K. Hendryx
Tyson J. Ririe
Lawrence DeLuca
Russell A. Chipman

Retinal oximeter for the blue-green oximetry technique

Kurt R. Denninghoff,[a] **Katarzyna B. Sieluzycka,**[b] **Jennifer K. Hendryx,**[b] **Tyson J. Ririe,**[b] **Lawrence DeLuca,**[a] **and Russell A. Chipman**[b]

[a]University of Arizona, Department of Emergency Medicine and College of Optical Sciences, 1609 North Warren Avenue, Room 116, Tucson, Arizona 85724-5057

[b]University of Arizona, College of Optical Sciences, 1630 East University Boulevard, Tucson, Arizona 85721

Abstract. Retinal oximetry offers potential for noninvasive assessment of central venous oxyhemoglobin saturation (SO_2) via the retinal vessels but requires a calibrated accuracy of $\pm 3\%$ saturation in order to be clinically useful. Prior oximeter designs have been hampered by poor saturation calibration accuracy. We demonstrate that the blue-green oximetry (BGO) technique can provide accuracy within $\pm 3\%$ in swine when multiply scattered light from blood within a retinal vessel is isolated. A noninvasive on-axis scanning retinal oximeter (ROx-3) is constructed that generates a multiwavelength image in the range required for BGO. A field stop in the detection pathway is used in conjunction with an anticonfocal bisecting wire to remove specular vessel reflections and isolate multiply backscattered light from the blood column within a retinal vessel. This design is tested on an enucleated swine eye vessel and a retinal vein in a human volunteer with retinal SO_2 measurements of ~1 and ~65%, respectively. These saturations, calculated using the calibration line from earlier work, are internally consistent with a standard error of the mean of $\pm 2\% \, SO_2$. The absolute measures are well within the expected saturation range for the site (–1 and 63%). This is the first demonstration of noninvasive on-axis BGO retinal oximetry. © *2011 Society of Photo-Optical Instrumentation Engineers (SPIE)*. [DOI: 10.1117/1.3638134]

Keywords: biomedical optics; backscattering; multispectral imaging; reflectometry; spectroscopy; spatial filtering.

Paper 11346R received Jul. 5, 2011; revised manuscript received Aug. 19, 2011; accepted for publication Aug. 24, 2011; published online Oct. 3, 2011.

1 Introduction

Retinal oximetry, the measurement of oxygen saturation in retinal blood vessels, may provide insight into retinal health as well as provide a noninvasive surrogate for central or mixed venous oxygen saturation.[1–5] Disparities in oxygen utilization between the left and right eyes, such as those that occur in diabetic retinopathy, could be measured to screen for retinal disease as well as for monitoring responses to interventions and experimental treatments.[6,7]

Retinal venous oxygen saturation has been demonstrated to predictably decrease during hemorrhagic shock, to rise with resuscitation, and to correlate with central venous oxygen saturation.[2,3,8,9] Early goal-directed therapy (EGDT) for patients with severe sepsis—a resuscitation algorithm using physiologic end points, including central venous oxygen saturation—has been shown to increase the survival of these patients.[10,11] Despite the survival benefit, compliance with central line placement in EGDT remains a major stumbling block to widespread adoption of the protocol.[11,12] A noninvasive means of assessing venous oxygen saturation could improve compliance with EGDT.

Prior retinal oximeters have suffered from poor accuracy with error ranges from ± 5–17% saturation when multiple measures are made.[13–17] There are several sources that contribute to this variability, including background, path length, blood hematocrit, and vessel glints.[4,13,14,16,18–21] Recent work in this area has attempted to reduce the measurement variability by taking large averages of the saturation data across selected portions of the retinal veins, but retinal color maps of the nonaveraged saturation data clearly showed substantial measurement variations. Notwithstanding this variability, the averaged data demonstrated significant changes in the global mean venous saturation in response to oxygen respiration as well as retinal disease states.[22–25] We have demonstrated the use of a blue-green oximetry technique (BGO) that overcomes many of the primary sources of measurement variability in the retina. However, the method has previously only been demonstrated using intravitrial illumination, which used off-axis invasive illumination techniques.[1,4,26] Here we describe the design and initial testing of a prototype oximeter, the noninvasive on-axis scanning retinal oximeter (ROx-3), which combines the BGO technique with an optical system designed to reject the vessel glint while utilizing on-axis, noninvasive illumination.

2 Methods

2.1 Specular Vessel Glint

A primary concern in the ROx-3 optical system is attenuation of the specular vessel glint. When a small spot of laser light is directed onto a blood vessel in the eye, there are many possible paths it can traverse.[26–30] Two paths of particular interest for this discussion are: (*i*) light specularly reflected from the blood vessel (also known as a glint) and (*ii*) laterally scattered light that has interacted with the red blood cell–packaged hemoglobin in the vessel and scattered back out of the eye. Figure 1(a) shows

Address all correspondence to: University of Arizona, Department of Emergency Medicine and College of Optical Sciences, 1609 North Warren Avenue, Room 116, Tucson, Arizona 85724-5057; Tel: 520-626-1551; Fax: 520-626-2480; E-mail: kdenninghoff@aemrc.arizona.edu
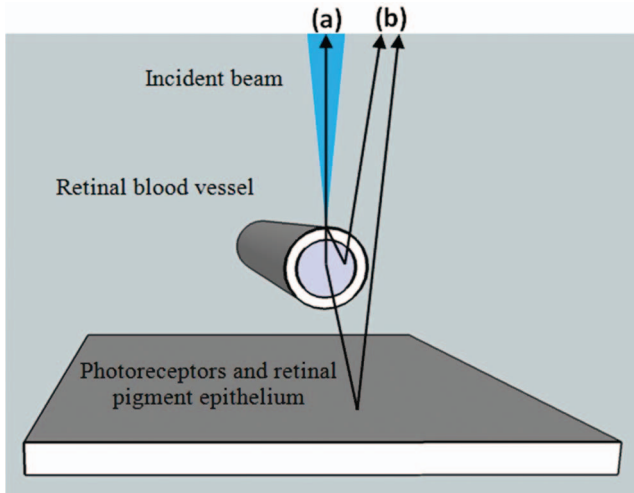
Fig. 1 Two light paths of interest when a retinal vessel is illuminated by a converging cone of light: (a) The glint, which reflects directly from the surface of the vessel and conveys little information about the oxygen saturation, and (b) laterally backscattered light that has interacted with red blood cells.

an example of the specular vessel glint path and Fig. 1(b) shows several examples of laterally scattered rays.

The glint is a specular reflection from the surface of the vessel. Because this light has not interacted with the hemoglobin inside the vessel, it does not contain information regarding oxygen saturation. This specular reflection frequently appears as a bright line down the center of vessels in retinal images.

The laterally backscattered light is the portion of the return signal that contains useful information about SO_2 (specifi-

cally "oxyhemoglobin" saturation, because we are looking at the spectral shift between oxyhemoglobin and deoxyhemoglobin). When a beam is incident on the retinal vessel, some of the light propagates into the blood vessel and interacts with hemoglobin inside the red blood cells, scattering in all directions. Some of this laterally scattered light exits the eye. If multiple monochromatic beams are sent into the eye, then the relative spectrum of this backscattered return signal is highly dependent on the oxygen saturation of the hemoglobin in the red blood cells.[25, 26] This signal may be many orders of magnitude dimmer than the specular reflection, making it difficult to efficiently collect the light containing oximetric information while rejecting the glint.

The ROx-3 was designed and built to selectively capture light scattered by red blood cells using on-axis illumination, a field stop, and an anticonfocal wire bisecting the field stop. This modified scanning laser ophthalmoscope improves on an earlier design by our group[17, 20, 31] by using mirrors rather than lenses to remove ghost reflections and an argon-ion multiline laser to generate the discrete wavelengths needed for BGO in this configuration. The illumination wavelength selection and image analysis exhibit the BGO technique.

2.2 Retinal Oximeter (ROx-3)

The ROx-3, optical layout shown in Fig. 2, is a modified confocal scanning laser ophthalmoscope that uses five monochromatic beams from a multiwavelength argon-ion laser (457.9, 476.5, 488, 496.5, and 514.5 nm) to sequentially scan the retina. The use of a single laser simplifies the system, and this wavelength range is sufficient for measuring SO_2 of 0–100% using the BGO minima technique.[1,4] An acousto-optic tunable filter (AOTF) (Crystal Technology AOTF PCAOM NI VIS 55–150 MHz) uses
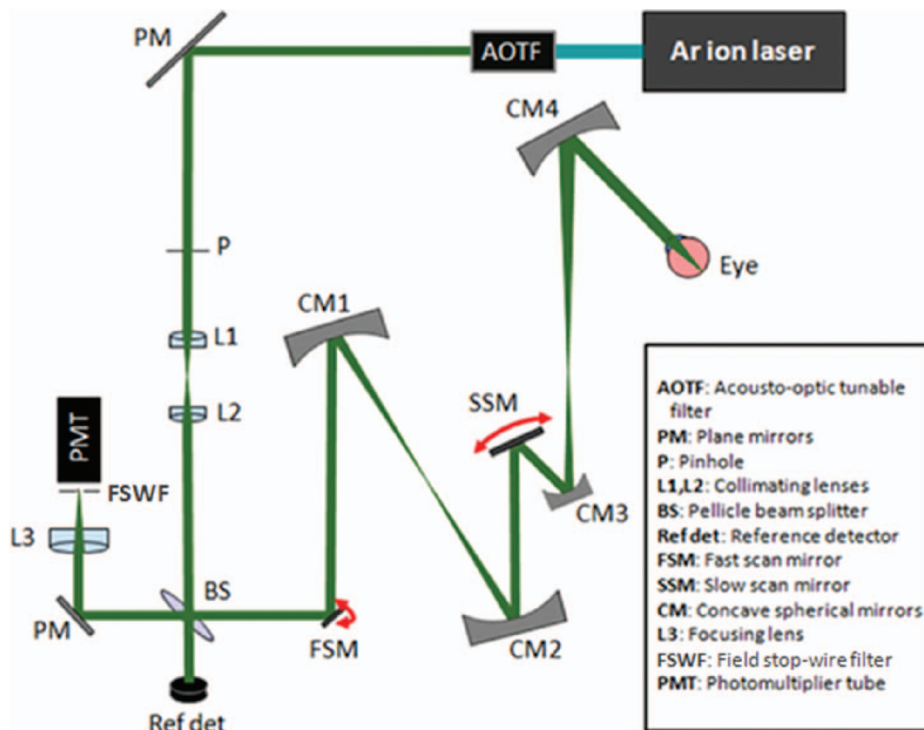
Fig. 2 Schematic of the ROx-3.
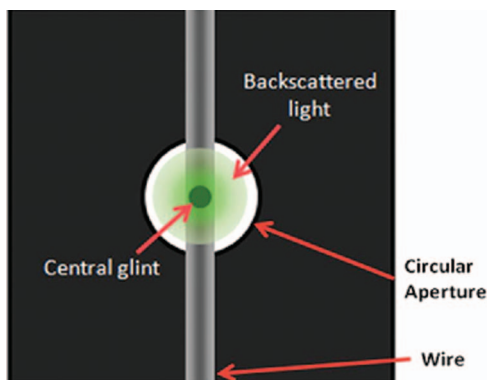
Fig. 3 Field stop-wire filter designed to reject the central vessel glint and transmit the backscattered light that contains hemoglobin information.

the timing of the fast-scan mirror (FSM) to sequentially switch line by line through each wavelength. A 1-mm-diam pinhole (P) following the AOTF ensures that no residual light from undesired wavelengths enters the system, and a set of adjustment lenses (L1, L2) ensures that the light is collimated. Four concave spherical mirrors (CM1–CM4) in an afocal arrangement direct the beam to the eye, where it is focused on the retina.

The light that scatters back out of the eye travels the illumination path in reverse. The portion transmitted by the pellicle beam splitter (BS) (Thorlabs BP208) is imaged onto the field stop-wire filter (FSWF) and detected by a photomultiplier tube (PMT) (Hamamatsu HC 125–01). The 8:92 (8% reflection, 92% transmission) pellicle beam splitter directs the majority of the return light to the PMT. Figure 3 shows how the confocal filter rejects the majority of the specular vessel glint and collects the backscattered light. The confocal filter is a 240-μm wire centered on a 2-mm-diam field stop placed at an image plane (at which the magnification is $\sim$10), just in front of the PMT. The material around the field stop rejects unwanted stray light coming from the optical system, the anterior chamber of the eye, and the vitreous humor. The central blocking wire rejects much of the light directly reflected back into the collection pathway by the structures anterior to the blood column at the scan site. The light that returns to the detector through the filter is primarily multiply scattered light from the blood within the vessel.

A two-dimensional image is generated by confocal scan mirrors and captured by a frame grabber (Foresight Imaging I-50 HSN). The laser beam is raster scanned over part of the retina by a FSM scanning vertically, and a slow-scan mirror (SSM) scanning horizontally. The scan mirrors descan the light returning out of the eye, which is focused onto the confocal filter. The concave mirrors CM1–CM4 image both scan mirrors onto the pupil. This allows the beam to be scanned across the retina without vignetting by using the iris as the pivot for the scans. The frame-grabber board uses sync pulses from the scan mirrors to generate an image with 10-bit depth resolution. The SSM controller triggers the start of each frame at a rate of 10 Hz. A full image is captured every half-cycle, in 50 ms using the FSM for bidirectional scanning. The FSM controller simultaneously triggers the AOTF wavelength switching at the start and end of each row of pixels (a switching rate of 8 kHz), creating an interlaced multiwavelength image. The data analysis relies on comparing

the return signal at different wavelengths to determine the oxygen saturation. This technique results in a slight shift between corresponding lines at each wavelength, but at these rates, only a small fraction of images must be discarded due to saccades or vessel motion. The area scanned by the ophthalmoscope is easily adjusted by increasing the angle of the scan mirrors. The device is designed to create images of a (3×3)-mm portion of the retina during targeting (10-deg arc). During measurements, the scan area is decreased to 0.5×0.5 mm (1.68-deg arc). The movement along the retina from line to line at the center of the image when in measurement mode is $\sim$0.625 μm or 3.75 μm for a complete five-wavelength line set with blank (0.013-deg arc). Two preliminary tests have been performed to assess the functionality of the ROx-3: one on an enucleated swine eye and a second on a human eye.

2.3 Testing the ROx-3 on an Enucleated Swine Eye

Enucleated swine eyes, with their easily observable blood vessels, are a convenient sample for testing an oximeter.[32] They are inexpensive, readily available, and provide a good model of the human eye.[33] They are also useful for preliminary testing before performing live swine or human eye studies with their requirements for a team of doctors, technicians, and associated costs. The living retina continues to remove oxygen from the vessels for several hours after enucleation, making the saturation of the hemoglobin in these vessels near 0%.[34]

An enucleated swine eye was obtained from the University of Arizona Meat Laboratory. Immediately on pickup, the eye was immersed in a balanced saline solution (BSS) of pH 7.4 and set on ice. Throughout the experiment, the cornea was periodically washed with the BSS to prevent opacification. In order to secure the eye for scanning without distorting its shape, the eye was mounted in a Styrofoam holder using cyanoacrylate and aligned until a retinal vessel was visible, and images were captured with the oximeter.

2.4 Testing the ROx-3 on a Human Eye

After successful scanning of the enucleated swine eye, scans were made of the eye of a healthy adult volunteer. The laser power at each wavelength was measured with a calibrated silicon detector to ensure that it was <30 μW. This power level has been shown to be within the safety limit for Class I laser devices, as defined by ANSI Z136.1 "Safe Use of Lasers."[35] The subject aligned his head in the proper position, an image was acquired with the ROx-3, and the subject was allowed to move his head (during which time the laser was not directed into his eye). This acquisition process was repeated three times. The experimental protocol was approved by the University of Arizona Institutional Review Board.

2.5 Data Analysis

Though there is a change in instrument geometry, we are fundamentally collecting the same light information as that gathered via intravitreal illumination[1,26] because we are employing the FSWF to block the central glint. Therefore, we can employ the same analysis techniques. The approximations for light paths involved in retinal oximetry described by Denninghoff et al. lead

to the simplified equation for data analysis that is used here,[1]

$$\frac{R_v(\lambda)}{S_1(\lambda)} \approx \frac{\Theta(\lambda)}{R_r}, \tag{1}$$

where R_v is the flux collected from the vessel; S_1 is the flux collected from the avascular fundus adjacent to the vessel; Θ is the fraction of incident light that is scattered by the blood in the vessel, the vessel wall, and other structures into the collection angle; and R_r is the fraction of light reflected or scattered from the avascular retina, a measure of retinal reflectivity. R_v and S_1 are determined from the retinal images, and Θ is the signal containing the oxyhemoglobin spectrum. The retinal reflectivity is almost constant in the (457.9–514.5)-nm wavelength range relevant for the ROx-3 in both swine and human eyes.[1,36,37]

BGO is based on the shape of the relative optical density spectrum of hemoglobin[38] and is independent of hematocrit and vessel size.[1] Relative ODs were calculated from the ROx-3 images by

$$OD(\lambda) = -\log\left(\frac{R_v(\lambda)}{S_1(\lambda)}\right). \tag{2}$$

The $OD(\lambda)$ values for each image set were used to generate a spectrum for the blood in the vessel. This spectrum was fit to a parabola using the method of least squares and the minimum wavelength of the parabola, λ_{min}, was then determined.

Using the model empirically verified by Denninghoff et al.[1] to further verify this methodology, the measured optical density data with respect to wavelength are expected to fit a line of the form

$$OD(\lambda) = A\lambda^2 + (B+b)\lambda + (C+c), \tag{3}$$

where A, B, and C are coefficients for the optical density due to absorption, and b and c are coefficients for the optical density due to scattering.[4] This is equivalent to writing the total optical density as the sum of optical densities due to absorption and scattering as proposed by Steinke and Shepherd, respectively,[38]

$$OD(\lambda) = d(OD_A + OD_S). \tag{4}$$

In this study, the total $OD(\lambda)$ was measured directly and the value OD_A for a given saturation is calculated using values reported in the literature and the effective path length of light in the blood calculated.[39] The effective path length of light into the vessel is the value d, and $OD_S(\lambda)$ was a line with a negative slope leading to a rightward shift in the BGO calibration line when blood was studied in transmission.[4] Subsequently, when we used intravitreal illumination to study retinal blood vessels in reflection, the calibration line was shifted in the opposite direction.[1]

The calibration line relating the λ_{min} to SO_2 calculated for swine retinal arteries using intravitreal illumination by Denninghoff et al.[1] was

$$\%SO_2 \approx 3.03 \times \lambda_{min} - 1421.21. \tag{5}$$

Using standard error of the mean (SEM), the error in λ_{min} ($SEM_{\lambda_{min}}$) therefore relates to the error in $\%SO_2$ ($SEM_{\%SO_2}$) by

$$SEM_{\%SO_2} = 3.03 \times SEM_{\lambda_{min}}. \tag{6}$$
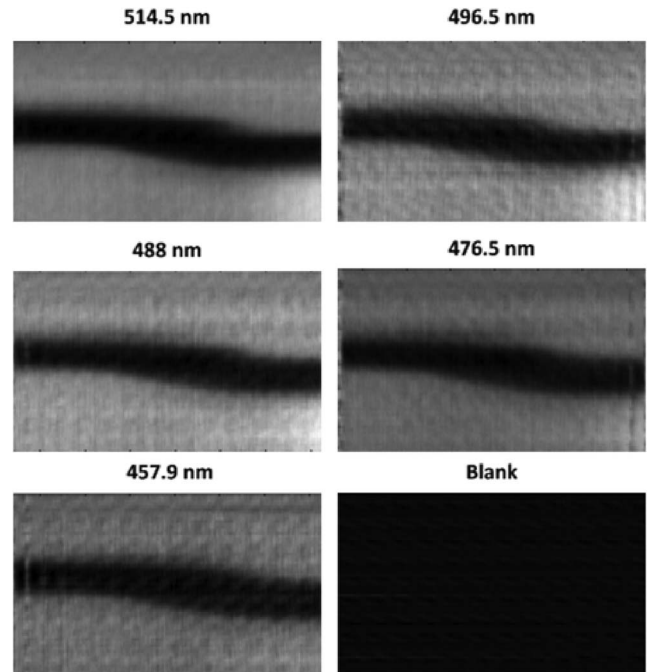
Fig. 4 Deinterlaced images of swine retinal vessel at five wavelengths and a blank.

We use this intravitreal illumination calibration line to roughly estimate the SO_2 work; however, a new calibration line is needed to properly evaluate the SO_2 measurements. However, the only change in the line is expected to be the intercept,[1] indicating that the $SEM_{\%SO_2}$ as calculated above is the true error in the SO_2 measurement.

3 Results

We obtained three interlaced images of swine retinal vessels in order to demonstrate the ability to consistently capture retinal vessel images without glints using this device. Figure 4 shows deinterlaced monochromatic images of a swine retinal vessel captured with the ROx-3. We only obtained one interlaced image of a human retinal vessel due to the discomfort to the volunteer during the targeting process using blue-green wavelengths. An infrared targeting system is being added to the design to alleviate this issue.

An important result of this study is the fact that there is no glint present in the images. Figure 5(a) shows typical intensity profiles of light returned from single scans across a swine vessel and, in Fig. 5(b), across a human vein. If a glint were present, then there would be an intensity spike near the center of the vessel profile. The human vein shows more noise because it was acquired at a lower light level than that used on the swine eye.

The calculated relative optical densities of the respective vessels are plotted against wavelength in Fig. 6. It was determined from Fig. 6(a) that the swine retinal vessels had minimum wavelength values of 468.5 ± 0.5 nm. From Fig. 6(b), the minimum wavelength value of the human vein was found to be 488.1 ± 0.8 nm.

We used our data from the swine and human eyes, the model equation for absorption, and scattering loss of light interacting with blood developed by Steinke and Sheppard,[38] and the BGO
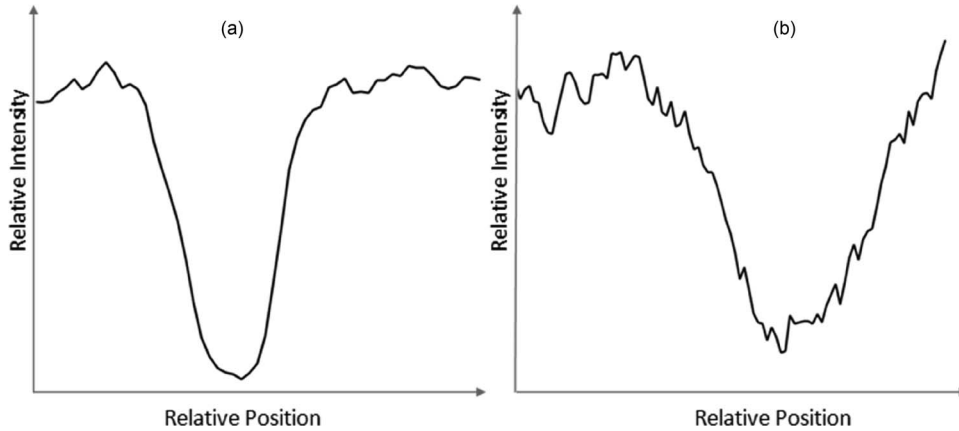
Fig. 5 Intensity profiles of (a) swine vessel and (b) human vein cross sections demonstrating the absence of significant glints.

calibration line determined for backreflected light in the eye from our earlier work[4] to solve for the apparent path length and apparent scattering component of the return signal seen using the ROx-3. The apparent path length (round trip) in blood was 48.59 μm in the swine eye and 40.55 μm in the human eye. The data displayed in Fig. 7 demonstrate that the scattering component of the return signal in both the human and swine eye is linear, has a positive slope, and the intercept is negative.

4 Discussion

The tissues of the eye continue to extract oxygen for several hours after enucleating the globe stops the supply of oxygenated blood, making the oxyhemoglobin saturation of the blood that remains in the swine retinal veins very near zero. Also, the human retinal vein oxyhemoglobin saturation is thought to be ~60%.[1,13,14,16,27,40,41] We estimated the oxyhemoglobin saturation in the enucleated swine retinal vein and in the *in vivo* human retinal vein using the calibration line from our intravitreal retinal illumination experiments[1] and the measured minima in Fig. 6. The calculated oxyhemoglobin saturation in the enucleated swine vessel was very near 0 as expected ($-1 \pm 2.0\%$ Sat), and the human vein oxyhemoglobin saturation ($63 \pm 2.3\%$ Sat) was also in the range reported elsewhere.[1,13,14,16,27,40,41]

4.1 On-Axis Blue-Green Oximetry and Removal of the Retinal Vessel Glint

Much of our efforts to provide calibrated blood hemoglobin spectroscopic measurements from the retina using on-axis illumination of the eye has been focused on finding ways to capture multiply scattered light from the retinal vessels while at the same time rejecting glints. The central glint does not appear in the swine images shown in Fig. 4 nor in the swine and human vessel profiles shown in Fig. 5, demonstrating that on-axis illumination can be used with a confocal field stop-wire filter to collect backscattered light and reject the specular vessel glint.

Our prior work showed that background, light path length, blood hemoglobin concentration, and other variations in measurements were independent of wavelength in the spectral range used for BGO when the glint was removed using invasive off-axis illumination.[1,26] Similarly, the optical light filtration used in the ROx-3 appears to overcome these challenges.

4.2 Oxygen Saturation Error

The uncertainty in determining SO_2 can be estimated by using the uncertainty in λ_{min} and the observation that the error in the linear relationship between λ_{min}, and SO_2 for all three geometries and samples determined previously has been 3% saturation
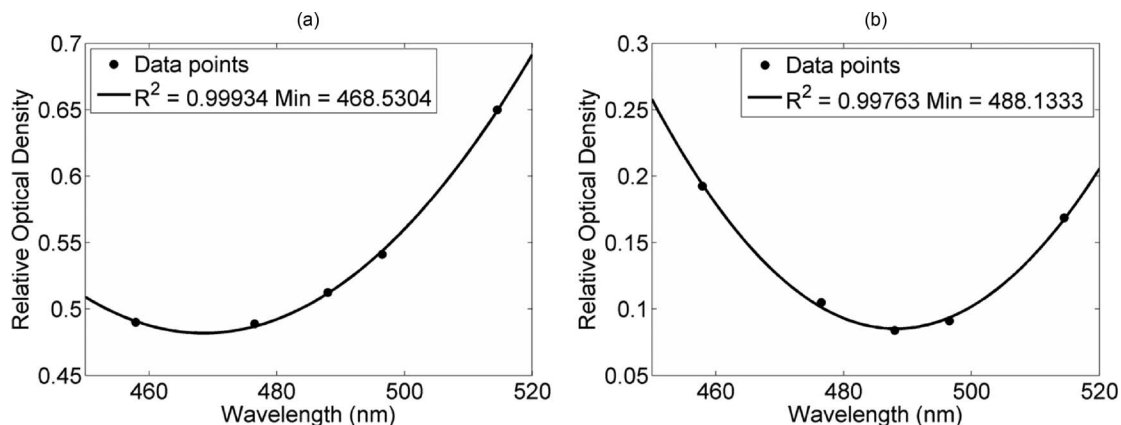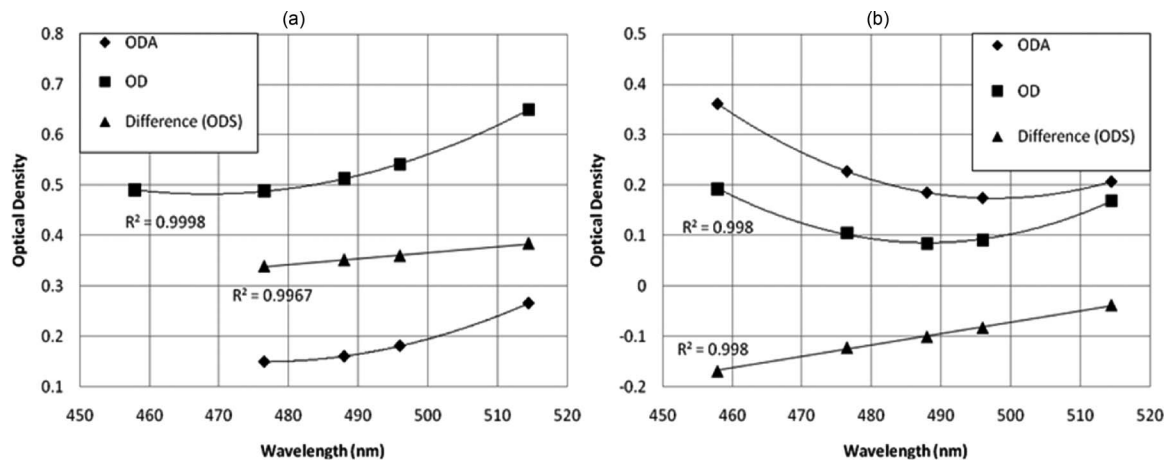

Fig. 6 Relative optical density versus wavelength with parabolic fit for (a) the swine retinal vessel and (b) the human vein.

Fig. 7 Plots comparing OD_A, OD_S, and OD for (a) the swine eye and (b) human eye. OD_A is calculated using [Hb] = 15 g/dL, extinction coefficients from Zijlstra et al. (Ref. 39), and the respective SO_2 values reported in this paper.

per 1 nm.[1,4,26,39] Using this relationship, the maximum error in λ_{min} from our human vein data of ± 0.8 nm corresponds to $\pm 2.3\%$ oxyhemoglobin saturation. The uncertainty of the measurements made using the ROx-3 is in the range we measured elsewhere and what we need for testing the potential use of a retinal oximeter clinically.

4.3 Backscattering of Light from the Eye in the Blue-Green Spectral Range

In our earlier work evaluating the use of the BGO technique in hemoglobin solutions[4,40] and blood in transmission,[1,26] we calculated the scattering component of the loss of light using the model equation developed by Steinke and Sheppard.[38] The scattering component was linear with wavelength, had a negative slope, and had a positive intercept.[4] Using a similar approach, we calculated the apparent path length through the blood and the scattering component for each wavelength. We found that the scattering was now a gain (negative intercept) with a positive slope. This is to be expected because the return light would be zero if there was no backscattering in the eye.

5 Conclusions

The saturation values calculated using the calibration line determined in our previous swine experiments gives us values for saturation that are in the expected range, and the errors of the measurements determined from the data are similar to previous work done by our group using BGO. The present device seems to successfully overcome the problems associated with on-axis scanning laser oximetry, including poor calibration, high local measurement error, and sensitivity to the amplitude of the vessel glint.

Here we report the first noninvasive *in vivo* application of blue-green oximetry to retinal vessels in the human eye using a modified confocal scanning laser ophthalmoscope (ROx-3). The ROx-3 eliminated the central vessel glint seen with prior devices and had measurement errors similar to prior invasive or *in vitro* tests using BGO. Further study is needed to characterize the calibration relationship between λ_{min} and SO_2 when the ROx-3 is used in swine and humans.

References

1. K. R. Denninghoff, D. A. Salyer, S. Basavanthappa, R. I. Park, and R. A. Chipman, "Blue-green spectral minimum correlates with oxyhemoglobin saturation *in vivo*," *J. Biomed. Opt.* **13**(5), 054059 (2008).
2. M. H. Smith, K. R. Denninghoff, L. W. Hillman, and R. A. Chipman, "Oxygen saturation measurements of blood in retinal vessels during blood loss," *J. Biomed. Opt.* **3**(3), 296–303 (1998).
3. K. R. Denninghoff, M. H. Smith, R. A. Chipman, L. W. Hillman, P. M. Jester, C. E. Hughes, F. Kuhn, and L. W. Rue, "Retinal large vessel oxygen saturations correlate with early blood loss and hypoxia in anesthetized swine," *J. Trauma-Injury Infect. Crit. Care* **43**(1), 29–34 (1997).
4. K. R. Denninghoff, R. A. Chipman, and L. W. Hillman, "Blood oxyhemoglobin saturation measurements by blue-green spectral shift," *J. Biomed. Opt.* **12**(3), 034020 (2007).
5. J. M. Beach, J. S. Tiedeman, M. F. Hopkins, and Y. S. Sabharwal, "Multispectral fundus imaging for early detection of diabetic retinopathy," *Proc. SPIE* **3603**, 114 (1999).
6. R. F. Gariano and T. W. Gardner, "Retinal angiogenesis in development and disease," *Nature* **438**(7070), 960–966 (2005).
7. G. Michelson and M. Scibor, "Intravascular oxygen saturation in retinal vessels in normal subjects and open-angle glaucoma subjects," *Acta Ophthalmol. Scand.* **84**(3), 289–295 (2006).
8. K. R. Denninghoff, M. H. Smith, A. Lompado, and L. W. Hillman, "Retinal venous oxygen saturation and cardiac output during controlled hemorrhage and resuscitation," *J. Appl. Physiol.* **94**(3), 891–896 (2003).
9. K. R. Denninghoff, M. H. Smith, L. W. Hillman, D. Redden, and L. W. Rue, "Retinal venous oxygen saturation correlates with blood volume," *Acad. Emerg. Med.* **5**(6), 577–582 (1998).
10. E. Rivers, B. Nguyen, S. Havstad, J. Ressler, A. Muzzin, B. Knoblich, E. Peterson, and M. Tomlanovich, "Early goal-directed therapy in the treatment of severe sepsis and septic shock," *New Engl. J. Med.* **345**(19), 1368–1377 (2001).
11. L. Stoneking, K. R. Denninghoff, L. DeLuca, S. Keim, and B. Munger, "Sepsis bundles and compliance with clinical guidelines," *J. Intens. Care Med.* **26**(3), 172–182 (2011).
12. D. J. Carlbom and G. D. Rubenfeld, "Barriers to implementing protocol-based sepsis resuscitation in the emergency department – results of a national survey," *Crit. Care Med.* **35**(11), 2525–2532 (2007).
13. F. C. Delori, "Noninvasive technique for oximetry of blood in retinalvessels," *Appl. Opt.* **27**(6), 1113–1125 (1988).
14. J. B. Hickam, R. Frayser, and J. C. Ross, "A study of retinal venous blood oxygen saturation in human subjects by photographic means," *Circulation* **27**(3), 375–385 (1963).

15. M. Hammer, T. Riemer, W. Vilser, S. Gehlert, and D. Schweitzer, "A new imaging technique for retinal vessel oximetry: principles and first clinical results in patients with retinal arterial occlusion and diabetic retinopathy," *Proc. SPIE* **7163**, 71630P (2009).

16. D. Schweitzer, M. Hammer, J. Kraft, E. Thamm, E. Konigsdorffer, and J. Strobel, "*In vivo* measurement of the oxygen saturation of retinal vessels in healthy volunteers," *IEEE Trans. Biomed. Eng.* **46**(12), 1454–1465 (1999).

17. M. H. Smith, "Oximetry of blood in retinal vessels," PhD Thesis, University of Alabama in Huntsville, Ann Arbor (1996).

18. M. H. Smith, K. R. Denninghoff, A. Lompado, J. B. Woodruff, and L. W. Hillman, "Minimizing the influence of fundus pigmentation on retinal vessel oximetry measurements," *Proc. SPIE* **4245**, 135–145 (2001).

19. F. C. Delori and K. P. Pflibsen, "Spectral reflectance of the human ocular fundus," *Appl. Opt.* **28**(6), 1061–1077 (1989).

20. A. Lompado, M. H. Smith, L. W. Hillman, and K. R. Denninghoff, "Multispectral confocal scanning laser ophthalmoscope for retinal vessel oximetry," *Proc. SPIE* **3920**, 67–73 (2000).

21. N. M. Anderson and P. Sekelj, "Light-absorbing and scattering properties of non-haemolysed blood," *Phys. Med. Biol.* **12**(2), 173–184 (1967).

22. S. H. Hardarson and E. Stefansson, "Oxygen saturation in branch retinal vein occlusion," *Acta Ophthalmol.* (2011) (online early view).

23. S. H. Hardarson and E. Stefansson, "Oxygen saturation in central retinal vein occlusion," *Am. J. Ophthalmol.* **150**(6), 871–875 (2010).

24. S. H. Hardarson, M. S. Gottfredsdottir, G. H. Halldorsson, R. A. Karlsson, J. A. Benediktsson, T. Eysteinsson, J. M. Beach, A Harris, and E. Stefansson, "Glaucoma filtration surgery and retinal oxygen saturation," *Invest. Ophthalmol. Vis. Sci.* **50**(11), 5247–5250 (2009).

25. S. H. Hardarson, A. Harris, R. A. Karlsson, G. H. Halldorsson, L. Kagemann, E. Rechtman, G. M. Zoega, T. Eysteinsson, J. A. Benediktsson, A. Thorsteinsson, P. K. Jensen, J. Beach, and E. Stefansson, "Automatic retinal oximetry," *Invest. Ophthalmol. Vis. Sci.* **47**(11), 5011–5016 (2006).

26. D. Salyer, N. Beaudry, S. Basavanthappa, K. Twietmeyer, M. Eskandari, K. Denninghoff, R. Chipman, and R. Park, "Retinal oximetry using intravitreal illumination," *Curr. Eye Res.* **31**(7), 617–627 (2006).

27. A. J. Cohen and R. A. Laing, "Multiple-scattering analysis of retinal blood oximetry," *IEEE Trans. Biomed. Eng.* **23**(5), 391–400 (1976).

28. M. Hammer, S. Leistritz, L. Leistritz, and D. Schweitzer, "Light paths in retinal vessel oxymetry," *IEEE Trans. Biomed. Eng.* **48**(5), 592–598 (2001).

29. M. H. Smith, K. R. Denninghoff, A. Lompado, and L. W. Hillman, "Effect of multiple light paths on retinal vessel oximetry," *Appl. Opt.* **39**(7), 1183–1193 (2000).

30. A. Lompado, M. H. Smith, L. W. Hillman, and K. R. Denninghoff, "In-plane scatterometry of small caliber blood column," *Opt. Diagnost. Biol. Fluids V* **3923**(1), 44–53 (2000).

31. L. C. Heaton, M. H. Smith, K. R. Denninghoff, and L. W. Hillman, "Handheld four-wavelength retinal vessel oximeter," *Ophthalm. Technol. X* **3908**(1), 227–233 (2000).

32. D. A. Salyer, K. Twietmeyer, N. Beaudry, S. Basavanthappa, R. I. Park, and R. Chipman, "*In vitro* multispectral diffuse reflectance measurements of the porcine fundus," *Invest. Ophthalmol. Vis. Sci.* **46**(6), 2120–2124 (2005).

33. L. Deschaepdrijver, P. Simoens, L. Pollet, H. Lauwers, and J. J. Delaey, "Morphological and clinical-study of the retinal circulation in the miniature pig. B. fluorescein angiography of the retina," *Exp. Eye Res.* **54**(6), 975–985 (1992).

34. A. Ames and F. Nesbett, "*In vitro* retina as an experimental-model of the central nervous-system," *J. Neurochem.* **37**(4), 867–877 (1981).

35. American National Standards Institute, "ANSI Standard for safe use of lasers," ANSI Z136.1–2007 (2007).

36. D. A. Salyer, K. R. Denninghoff, N. Beaudry, S. Basavanthappa, R. I. Park, and R. A. Chipman, "Diffuse spectral fundus reflectance measured using subretinally placed spectralon," *J. Biomed. Opt.* **13**(4), 044004 (2008).

37. J. Schwiegerling, *Field Guide to Visual and Ophthalmic Optics*, p. 109, SPIE Press, Bellingham, WA (2004).

38. J. M. Steinke and A. P. Shepherd, "Diffusion model of the optical absorbance of whole blood," *J. Opt. Soc. Am. A* **5**(6), 813–822 (1988).

39. W. G. Zijlstra, A. Buursma, and O. W. van Assendelft, *Visible and Near Infrared Absorption Spectra of Human and Animal Haemoglobin*, VSP BV, Netherlands (2000).

40. S. H. Hardarson, S. Basit, T. E. Jonsdottir, T. Eysteinsson, G. H. Halldorsson, R. A. Karlsson, J. M. Beach, J. A. Benediktsson, and E. Stefansson, "Oxygen saturation in human retinal vessels is higher in dark than in light," *Invest. Ophthalmol. Visual sci.* **50**(5), 2308–2311 (2009).

41. J. M. Beach, K. J. Schwenzer, S. Srinivas, D. Kim, and J. S. Tiedeman, "Oximetry of retinal vessels by dual-wavelength imaging: calibration and influence of pigmentation," *J. Appl. Physiol.* **86**(2), 748–758 (1999).